Functional form of the Parisi overlap distribution for the three-dimensional Edwards-Anderson Ising spin glass

Bernd A. Berg,[1,2,*] Alain Billoire,[2,†] and Wolfhard Janke[3,‡]

[1]*Department of Physics, The Florida State University, Tallahassee, Florida 32306*
[2]*CEA/Saclay, Service de Physique Théorique, 91191 Gif-sur-Yvette, France*
[3]*Institut für Theoretische Physik, Universität Leipzig, 04109 Leipzig, Germany*

Recently, it has been conjectured that the statistics of extremes is of relevance for a large class of correlated systems. For certain probability densities this predicts the characteristic large x falloff behavior $f(x) \sim \exp(-ae^x)$, $a > 0$. Using a multicanonical Monte Carlo technique, we have measured the Parisi overlap distribution $P(q)$ for the three-dimensional Edward-Anderson Ising spin glass at and below the critical temperature We find that a probability distribution related to extreme-order statistics gives an excellent description of $P(q)$ over about 80 orders of magnitude.

PACS number(s): 75.10.Nr, 75.40.Mg, 75.50.Lk

The three-dimensional (3D) Edwards-Anderson [1] Ising (EAI) spin-glass model is a prototype of a disordered system, for which conflicting constraints create a rough free-energy landscape. Such systems are of importance for the understanding of a wide range of phenomena in physics, chemistry, biology, and computer science. The overlap q between two replicas of the EAI model serves as an order parameter. Its probability density $P(q)$ is, therefore, a quantity of central physical interest. More than 20 years ago, Parisi succeeded to calculate $P(q)$ in the mean-field approximation [2]. However, for 3D physical systems the precise form of $P(q)$ in the spin-glass phase, and the very nature of this phase, have remained a subject of debate [3,4].

We use a multicanonical Monte Carlo (MC) technique [5,6] for calculating $P(q)$ numerically, specifically tailored for the exponentially small tail of the distribution where we can measure probabilities as small as 10^{-160} with good precision. In this paper we show that, at the critical point, a modification of Gumbel's first asymptote (introduced below) gives a perfect description of the data over about 80 orders of magnitude, and the agreement appears to continue below the critical temperature. Although the detailed relationship between extreme-order statistics and the EAI model remains to be understood, it is certainly quite rare that a physical formula has been tested over such a large range.

The statistics of extremes was pioneered by Fréchet, Fisher and Tippet, and von Mises. A standard result [7,8], due to Fisher and Tippet, Kawata, and Smirnov, is the universal distribution of the first, second, third, etc. smallest of a set of N independent identically distributed random numbers. For an appropriate, exponential decay of the random number distribution, their probability densities are given by

$$f_a(x) = C_a \exp[a(x - e^x)] \tag{1}$$

in the limit of large N. The exponent a takes the values a $=1,2,3,\ldots$, corresponding, respectively, to the first, second, third, etc. smallest random number of the set. x is a scaling variable, which shifts the maximum value of the probability density to zero, and $C_a = a^a/\Gamma(a)$ normalizes the integral over $f_a(x)$ to 1. In Gumbel's book [7] Eq. (1) is called the first asymptote, as it holds for the asymptotic extreme-order statistics of the first of altogether three different classes of random number distributions. In the last years a noninteger value of the exponent a received some attention. For the probability density of the magnetization of the 2D XY model Bramwell *et al.* [9,10] derived $a = \pi/2$ in the spin wave approximation and conjectured that this exponent describes, at least approximately, probability densities of a large class of correlated systems, including (besides the mentioned systems) turbulent flow problems, percolation models and some self-organized critical phenomena.

For disordered systems Bouchaud and Mézard [11] noted that a relationship to extreme order statistics is intuitively quite obvious. Namely, at low temperatures a disordered system will preferentially occupy its low-energy states, which are random variables due to the quenched exchange interactions of the system. Their investigation of the random-energy model shows that Gumbel's first asymptote with $a = 1$ corresponds to one-step replica symmetry breaking, and their conjecture of a relationship between extreme order statistics and disordered systems is certainly far more general. This, and the possible description of a broad range of correlated systems by the $a = \pi/2$ modification of Gumbel's first asymptote, has motivated us to analyze the overlap probability density of the EAI model at and below the critical point with respect to the large x falloff behavior of Eq. (1).

The energy function of the $J = \pm 1$ EAI spin-glass model is given by [1]

$$E = -\sum_{\langle ik \rangle} J_{ik} s_i s_k, \tag{2}$$

where the $s_i = \pm 1$ are the spins of the system and the sum is over the nearest-neighbor pairs of a cubic L^3 lattice with periodic boundary conditions. The coupling constants J_{ik} are

*Email address: berg@hep.fsu.edu
†Email address; billoir@spht.saclay.cea.fr
‡Email address: wolfhard.janke@itp.uni-leipzig.de
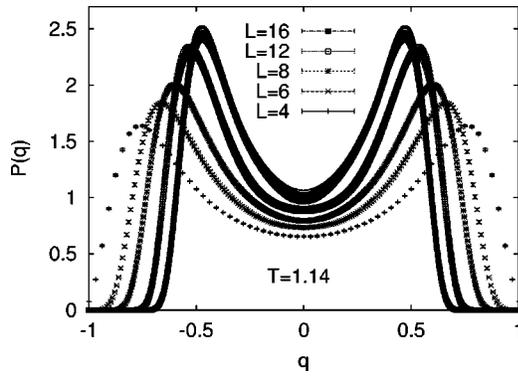
FIG. 1. Overlap probability densities $P_L(q)$ versus q for the EAI model on L^3 lattices at the critical temperature.

FIG. 2. Rescaled overlap probability densities for the EAI model on L^3 lattices at the critical temperature. In the lower part the deviation $P'_{16}(q') - P'_{\text{fit}}(q') \pm \triangle P'_{16}(q')$ of some $L=16$ data from the fit is shown. It has been shifted upwards by 0.2 to fit inside the figure.

quenched random variables, which take on the values ± 1, with equal probabilities. A set of coupling constants defines a realization $\mathcal{J} = \{J_{ik}\}$ of the system. The two-replica overlap (Parisi order parameter) is defined by

$$q = \frac{1}{L^3} \sum_{i=1}^{L^3} s_i^{(1)} s_i^{(2)}, \tag{3}$$

where the $s_i^{(1)}$ and $s_i^{(2)}$ are the spins of two copies (replica) of the realization $\mathcal{J}$ and the sum is over all sites. The overlap probability density is given by the average over the probability densities $P^{\mathcal{J}}(q)$ of all realizations

$$P_L(q) = \frac{1}{N_{\mathcal{J}}} \sum_{\mathcal{J}} P^{\mathcal{J}}(q), \tag{4}$$

where $N_{\mathcal{J}}$ is the number of realizations used and L is the lattice size. There is a long history of MC studies of this model (see [12–19] and references therein), which have led to a wealth of information. Here we introduce only two results.

(1) The model has a freezing transition at a finite temperature, which according to the most recent estimates [16,19] is consistent with $T_c = 1.14$.

(2) References [14–16,18] reported results that were consistent with a Kosterlitz-Thouless [20] (KT) type line of critical points below T_c, quite similar to the 2D XY model.

In our context, this is of interest in view of the description of this model by Eq. (1) with $a = \pi/2$ [9]. Note, however, that one of the most recent EAI investigations [19] claims to rule out the KT scenario.

At $T = 1.14$ we generated 8192 realizations for $L = 4$, 6, and 8; 1024 realizations for $L = 12$; and 256 realization for $L = 16$. Figure 1 shows our normalized $P(q)$ probability densities. Due to the MC method, the error bars of neighboring entries are strongly correlated. This results in smooth curves of varying thickness, which represents the error. The pearl of these data are the tails of the distributions, which (for $L = 16$) are accurate down to 10^{-160} (for $|q|$ towards 1). This is achieved by simulating the system in a ($\mathcal{J}$ dependent) statistical ensemble for which the distribution of q values is
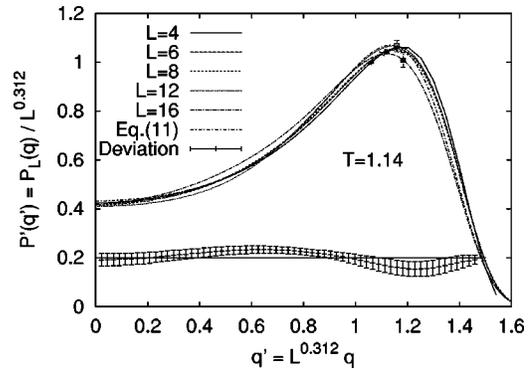
approximately flat [6], instead of using the Gibbs canonical ensemble. After the simulation, results for the Gibbs ensemble are obtained through an exact reweighting procedure. In this way computer simulations allow to probe easier into the extremes of materials than real experiments. Alongside with our data at the critical point, we analyze our data from our simulations [17,18] at $T = 1$, below the critical point. In that case we generated 8192 realizations for $L = 4$, 6, 8, and 640 realizations for $L = 12$. In the tails the data (for $L = 12$) at $T = 1$ are accurate down to 10^{-53}.

We first ask the question whether, up to finite-size corrections, the probability densities depicted in Fig. 1 scale. A method to investigate this is to plot $\sigma_L P_L(q)$ versus $(q - \hat{q}_L)/\sigma_L$, where $\hat{q}_L$ is the mean value of q with respect to the distribution $P_L(q)$ and σ_L is its standard deviation (here $\hat{q}_L = 0$ because the $P_L(q)$ are even functions). A visual inspection shows that the data scale indeed and we proceed to fit the standard deviations to the two-parameter form $\sigma_L = c_1 L^{-\beta/\nu}$ to obtain

$$\frac{\beta}{\nu} = 0.312(4), \quad Q = 0.32 \text{ for } T = 1.14, \tag{5}$$

and

$$\frac{\beta}{\nu} = 0.230(4), \quad Q = 0.99 \text{ for } T = 1. \tag{6}$$

Here the numbers in parentheses denote error bars with respect to the last digits and Q is the goodness of fit. For $T = 1.14$ we plot in Fig. 2 $P'(q') = P_L(q)/L^{\beta/\nu}$ versus $q' = L^{\beta/\nu} q$ and see that the five probability densities collapse onto a single curve. To enlarge the scale, we restrict ourselves to the $q \geq 0$ range. The (relative) error bars of the lines in Fig. 2 are the (relative) error bars of Fig. 1. Not to obscure the agreement, we include only one representative error bar for each lattices size, $L = 16, 12, \ldots$ from right to left in Fig. 2 (for $L \leq 8$ they are barely visible on the scale of the figure). For our data at $T = 1$ a similar analysis is already given in [18]. The small discrepancy in the estimates of the critical exponent β/ν (0.255 in [18] instead of 0.230) is due to using different methods of data analysis. Note that the error bars of

the β/ν estimates (5) and (6) reflect only the fluctuations of our two-parameter fit and additional (systematic) errors are expected from corrections to scaling.

Our aim is to relate the probability distribution of Fig. 2 to the first asymptote of extreme-order statistics Eq. (1). In the neighborhood of $x=0$ the expansion

$$x - e^x = -1 - \tfrac{1}{2}x^2 + O(x^3) \qquad (7)$$

holds. To get the position of the maximum of $P'(q')$ right, we have to choose

$$x = b(q' - q'_{max}), \qquad (8)$$

where q'_{max} is the $q'>0$ argument for which the probability density $P'(q')$ takes on its maximum value. We then have to find an exponent a to reproduce the data for $x = b(q' - q'_{max})>0$. For $x = b(q' - q'_{max})<0$, however, the behavior (1) cannot be quite correct. The reason is that the $x<0$ asymptotic behavior

$$\exp[ax] = \exp[a\,b(q' - q'_{max})] \qquad (9)$$

predicts, on a logarithmic scale, a constant slope a with decreasing x, while for the data of Fig. 2 the slope levels off and at $q'=0$ (i.e., $x = -bq'_{max}$) the derivative of $P'(q')$ becomes zero, what is impossible with Eq. (9). A simple solution is to replace the first x on the right-hand side of Eq. (1) by $c\tanh(x/c)$, where $c>0$ is a constant. For small x the Taylor expansion (7) still holds, while for large $|x|$ the hyperbolic tangent function $c\tanh(x/c)$ approaches quickly $\pm c$ [note that in the limit $c\to\infty$ the original form (1) is recovered]. For $x\to-\infty$ (practically already at $q'=0$) the thus modified Gumbel distribution becomes constant. Therefore, the symmetric expression for $P'(q')$ is obtained by multiplying the above construction with its reflection about the $q'=0$ axis

$$P'(q') = C \exp\left\{ a\left[c\tanh\left(+\frac{b}{c}(q' - q'_{max}) \right) \right.\right.$$

$$\left. - \exp[+b(q' - q'_{max})] \right] \Big\}$$

$$\times \exp\left\{ a\left[c\tanh\left(-\frac{b}{c}(q' + q'_{max}) \right) \right.\right.$$

$$\left.\left. - \exp[-b(q' + q'_{max})] \right] \right\}. \qquad (10)$$

Of course, the important large x behavior of Eq. (1) is not at all affected by our manipulations.

The calculation of the parameters a, b, c, and C is done by using the logarithm of Eq. (10). Starting values are determined by the following parts of the distribution: C by the height of the peak at $q'=q'_{max}$ (now off the maximum location by a tiny shift which can be neglected; in the fits we used $q'_{max}=1.135\,972$ for $T=1.14$ and $q'_{max}=1.115\,056$ for
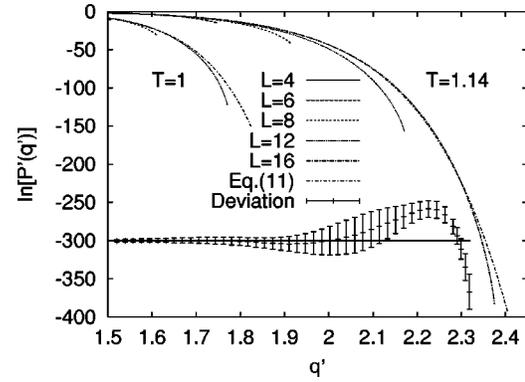
FIG. 3. Tails of the rescaled overlap probability densities of Fig. 2: $\ln[P'(q')]$ versus q'. For $T=1.14$ we show in the lower part the deviation $20[\ln P'_{16}(q') - \ln P'_{fit}(q') \pm \Delta \ln P'_{16}(q')]$ of some $L=16$ data from the fit, shifted downwards by 300.

$T=1$), a and b by the $q'>q'_{max}$ tails of the distribution and c by the value at $q'=0$. This allows to iterate to our final estimates

$$a = 0.448(40) \quad \text{for} \quad T=1.14, \qquad (11)$$

and

$$a = 0.446(37) \quad \text{for} \quad T=1. \qquad (12)$$

The nonuniversal coefficients are $b=5.35(11)$, $c=3.37(41)$, $C=7.55(88)$ for $T=1.14$, and $b=8.23(17)$, $c=4.48(43)$, $C=16.8(2.2)$ for $T=1$. The error bars rely on a jackknife analysis.

For $T=1.14$ our best fit to Eq. (10) is already included in Fig. 2. To demonstrate its quality we plot in the lower part of the figure the deviation from the fit for (a subset of) the $L=16$ data. Good consistency between the data and the fit is found over the plotted range of q'.

In Fig. 3, we follow the tails of our distributions by plotting $\ln[P'(q')]$ versus q' for $q'\geqslant 1.5$. Besides $T=1.14$, the results for $T=1$ are also included in this figure. On the scale of Fig. 3 the error bars are not visible. As in Fig. 2, we indicate the accuracy of the $L=16$ data for $T=1.14$ in the lower part of the figure. Figure 3 exhibits the finite-size effect, due to which, for q close to 1, the smaller lattices undershoot the larger ones. It is quite clear that something as this has to happen, because the data from each lattice size terminates at $q=1$, whereas Eq. (10) has no corresponding singularity. When calculating our fit parameters, we take this into account by restraining our use of data to $q'<2$, $\ln[P'(q')]>-43.4$ for the $T=1.14$, $L=16$ lattice, and to $q'<1.62$, $\ln[P'(q')]>-25.6$ for the $T=1$, $L=12$ lattice. The agreement of our fits with those data stretches then over considerably larger ranges. Statistically significant discrepancies of the $L=16$ data with the fit begin only around $\ln[P'(q')]=-200$. Discrepancies of the $T=1$, $L=12$ lattice with the fit are encountered around $\ln[P'(q')]=-35$. However, the $T=1.14$, $L=12$ data deviate already around $\ln[P(q')]=-10$ from the $L=16$ data. This is possible, because corrections to the $L^{0.312}$ scaling factor are not traced by the accu-

racy of our data (in particular $L=16$ has low statistics due to computer time limitations). Therefore, it is not entirely clear whether the large range, which we find for the agreement of the fit with our $L=16$ lattice, is to some extent a statistical accident. Taking it at face value, we have the remarkable range of $200/\ln(10) \approx 87$ orders of magnitude.

Our coefficient a differs from the 2D XY coefficient of Bramwell *et al.* [9], $a=\pi/2$. This means that the EAI and the 2D XY models are certainly in quite different universality classes of extreme-order statistics. However, the fact that both distributions can be described by it at all might help to explain the observed similarities. Our temperature $T=1$ is below the critical T_c, but with our lattice sizes it appears impossible to resolve the question, whether the here-reported behavior reflects the existence of a critical line below T_c or just the closeness of $T=1$ to T_c. Before comparing to extreme-order statistics, we [18] tried to fit the $q>q_{\max}$ tails of our distributions to the theoretical predictions that have been made [21–23] based on the replica mean-field approach. None of these fits was particularly good and even when pushing the adjustment of free parameters to their limits only small parts of the tails of our distributions could be covered.

In summary, we have presented strong numerical evidence that the Parisi overlap distribution of the EAI model can be described by Eq. (10). The excellent agreement over many decades suggests a deep relation to simple, but fundamental statistical properties, presumably also present in many other correlated systems. The detailed relationship between the EAI model and extreme-order statistics remains to be investigated and it is certainly a challenge to extend the work of Bouchaud and Mézard [11] to the more involved scenarios of the replica theory. On the other hand, it could be that replica symmetry breaking is not the driving mechanism of the EAI model phase transition and that our observations are rooted in general relations [9] between extreme-order statistics and certain universality classes of correlated systems.

[1] S.J. Edwards and P.M. Anderson, J. Phys. F: Met. Phys. **5**, 965 (1975).

[2] M. Mézard, G. Parisi, and M.A. Virasoro, *Spin Glass Theory and Beyond* (World Scientific, Singapore, 1987).

[3] D.S. Fisher and D.A. Huse, Phys. Rev. B **38**, 386 (1988).

[4] *Spin Glasses and Random Fields*, edited by A.P. Young (World Scientific, Singapore, 1997).

[5] B.A. Berg and T. Neuhaus, Phys. Rev. Lett. **68**, 9 (1992).

[6] B.A. Berg and W. Janke, Phys. Rev. Lett. **80**, 4771 (1998).

[7] E.J. Gumbel, *Statistics of Extremes* (Columbia University Press, New York, 1958).

[8] J. Galambos, *The Asymptotic Theory of Extreme Order Statistics*, 2nd ed. (Krieger, Malabar, FL, 1987).

[9] S.T. Bramwell *et al.*, Phys. Rev. Lett. **84**, 3744 (2000).

[10] S.T. Bramwell *et al.*, Phys. Rev. E **63**, 041106 (2001).

[11] J.-P. Bouchaud and M. Mézard, J. Phys. A **30**, 7997 (1997).

[12] A.T. Ogielski, Phys. Rev. B **32**, 7384 (1985).

[13] R.N. Bhatt and A.P. Young, Phys. Rev. B **37**, 5606 (1988).

[14] N. Kawashima and A.P. Young, Phys. Rev. B **53**, R484 (1996).

[15] D. Iñiguez, E. Marinari, G. Parisi, and J.J. Ruiz-Lorenzo, J. Phys. A **30**, 7337 (1997).

[16] M. Palassini and S. Caracciolo, Phys. Rev. Lett. **82**, 5128 (1999).

[17] B.A. Berg, A. Billoire, and W. Janke, Phys. Rev. B **61**, 12 143 (2000).

[18] W. Janke, B.A. Berg, and A. Billoire, in *Non-Perturbative Methods and Lattice QCD*, Proceedings of the International Workshop, China, 2000, edited by X.-Q. Luo and E.B. Gregory (World Scientific, Singapore, 2001), p. 242.

[19] H.G. Ballesteros *et al.*, Phys. Rev. B **62**, 14 237 (2000).

[20] J.M. Kosterlitz and D.J. Thouless, J. Phys. C **6**, 1181 (1973).

[21] S. Franz, G. Parisi, and M.A. Virasoro, J. Phys. I **2**, 1869 (1992).

[22] G. Parisi, F. Ritort, and F. Slanina, J. Phys. A **26**, 3775 (1993).

[23] J.C. Ciria, G. Parisi, and F. Ritort, J. Phys. A **26**, 6731 (1993).